Desalination and Water Treatment
www.deswater.com

doi: 10.5004/dwt.2018.21835

104 (2018) 225–233
February

Comparative study of the adsorption of paracetamol from aqueous solution on olive stones and date pits

Fatma Medjdoub*, Krim Louhab, Aksas Hamouche

Research Laboratory of Food Technology, Faculty of Engineering Sciences, Boumerdès University, 35000 Boumerdès, Algeria, Tel. +213 24911116; emails: fatma.medjdoub@yahoo.fr (F. Medjdoub), louhab_ka@yahoo.fr (K. Louhab), Tel. +213 551158145; email: aksas_ha@yahoo.fr (A. Hamouche)

Received 17 April 2017; Accepted 21 December 2017

ABSTRACT

The present study consists of comparing the retention of paracetamol dispersed in aqueous solutions by two different natural adsorbents commonly found in Algeria, namely olive stones (OS) and date pits (DP). Comparative study was carried out using adsorption parameters such as contact time, temperature and initial concentration of paracetamol. The kinetic study revealed that adsorption on both adsorbents follow the pseudo-second-order equation but the values of adsorption capacity, q_e, and the rate constant, k_2, are found to be 37.12 mg g^{-1} and 0.0128 g mg^{-1} min^{-1}, respectively, for OS, which are significantly higher than those obtained for DP which are 29.74 mg g^{-1} and 0.0032 mg g^{-1} min^{-1}, respectively, on the other hand, data of equilibrium has been well adjusted by the Langmuir isothermal model. The adsorption of paracetamol on these adsorbents is exothermic and spontaneous with $\Delta S° = -71.0$ J mol^{-1} K^{-1} and $\Delta H° = -30.4$ kJ mol^{-1} for OS and $\Delta S° = -10.2$ J mol^{-1} K^{-1} and $\Delta H° = -6.1$ kJ mol^{-1} for DP. The results indicate that the OS was more efficient with a removal percentage greater than 98% compared with the DP which is about 78%, these results are similar to those found by scanning electron microscopy in the OS which represent porous structure with a number of pores larger than those observed for DP and even the X-ray fluorescence analysis shows that the surface nature of OS contains a significant percentage of calcium contrary to DP which has a higher percentage in potassium.

Keywords: Adsorption; Paracetamol; Olive stones; Date pits; Comparative study

1. Introduction

The global concern for the presence of pharmaceutical compounds in water has increased dramatically in recent years [1], which is actually presenting, one of the most important environmental and public health problems [2]. These compounds that can be found in a drinking water [3,4] are detected in wastewater and surface water at levels of ng L^{-1} to μg L^{-1} [5,6]. In particular, paracetamol (PAC), also known as acetaminophen mostly consumed over the world, is analgesic and antipyretic [7] with or without medical prescription, [8] both of them are distinguished to be very toxic to the liver [9] with a potential risk of developing hepatitis [9].

Therefore, it is imperative to search for efficient and economically feasible procedures to improve water treatment. Olive stones (OS) and date pits (DP) are solid wastes from the oleic industry and the date pulp industry, respectively, produced on a large scale in Algeria with an olive oil patrimony valued at more than 32 million olive trees occupying about 383.443 hectare [10] and with a production date of nearly 790,000 tons per year according to the official website of the International Exhibition of the Dating of Biskra “SIDAB”, whose first edition was organized from 21 to 24 March 2015 in Biskra under the auspices of the Zibans Chamber of Commerce and Industry and the Algerian Chamber of Commerce and Industry [11].

In general, the use of OS and DP as natural adsorbents in adsorption processes is an interesting strategy to deal with the problem of elimination of this landfill wastes and its

---

* Corresponding author.

recycling. There are many studies in literature that included using OS and DP as adsorbents for dyes [11,12] and heavy metals elimination [13,14].

This study consists of making a comparative study between the OS and the DP as natural adsorbents in terms of efficiency of removal of PAC from aqueous solutions. From this perspective, a study of the kinetics, equilibrium and thermodynamics of the suppression of PAC was carried out and the most efficient adsorbent was olive stone.

2. Materials and methods

2.1. Reagents and materials

The olive stone was harvested from an oil mill in the north of Algeria and the DP were supplied by an industry in the south of Algeria. The adsorbents were washed with hot water and then with distilled water, after grinding, the adsorbents were impregnated in hexane (Sigma-Aldrich, 99%) at room temperature for 24 h to extract any type of oil and impurities, and then washed until the pH is between 6.5 and 7. The mixture was then heat-treated in a programmable muffle furnace (Stuart mod SF3/S) during 60 min at 700°C, and then characterized by Fourier transform infrared spectroscopy (FTIR), scanning electron microscopy (SEM) and X-ray fluorescence (μFRX). The PAC (molecular weight = 151.2 g mol^{-1}; chemical formula = $C_8H_9NO_2$; pKa = 9.5 = 4.2; hydrophbicity = logK_{ow} ~ 0.46) [15] was procured from the bio-pharma SAIDAL, Algeria, and all solutions were prepared with distilled water.

2.2. Characterization of adsorbents

SEM (600 Quanta/EDAX) at 25 kV and energy dispersive X-ray spectrometry were used to observe the morphology of the adsorbents.

Main functional groups were determined by an infrared spectrophotometer transform infrared FTIR (Fourier, Thermo Nicolet typical 6700) .The spectra were performed between 400 and 4,000 cm^{-1} (64 scans) using the KBr pellet method.

μFRX is a non-destructive, qualitative and quantitative elemental analysis technique for any sample (solid, liquid or gaseous). The device used is Horiba; XGT model 5000, with a rhodium X-ray source.

2.3. Adsorption experiments

The kinetics and the equilibrium adsorption process were conducted at different concentrations of PAC (20, 40, 60, 80 and 100 μM) using 10 mg of heat-treated coal mixed with 25 mL of the PAC solution. The solution was then stirred at a constant speed of 300 rpm for 3 h on electromagnetic stirrers at a pH = 6 at room temperature (20°C ± 2°C). After stirring, the adsorbate was separated from the solution by filtration through a 0.45 μm filter paper of cellulose and the PAC residual concentration was analyzed by UV–vis spectrophotometry (SHIMADZU, UV 1800, 240 V) at the wavelength of 243 nm. PAC uptake (q_t, in mg g^{-1}) was calculated using Eq. (1):

$$q = \frac{\left(C_i - C_t\right)\times V}{m} \tag{1}$$

where C_i (mg L^{-1}) and C_t are the concentrations of PAC at time $t = 0$ and at time t, respectively, V (L) is the volume of solution and m (g) is the amount of adsorbent added.

In order to determine the effect of initial pH of the two sorbents performance, experiments at different initial pH were carried out. For these experiments, 10 mg of the sorbents was thoroughly mixed with PAC solution (25 mg L^{-1}) at different initial pH within the range of 2.0–11.0 for 3 h and the pH of the solutions was adjusted with either HCl (1 M) or NaOH (1 M).

The thermodynamics and the effect of temperature on the adsorption of PAC were studied using three different temperatures (20°C, 30°C and 40°C) with initial concentrations of 100 μM using an ultrathermostatic bath for up to 3 h.

3. Results and discussion

3.1. SEM analysis

SEM analysis (Fig. 1) revealed that the surface texture of the OS had a porous structure, holes and small openings on the surface with a number of larger pores than those observed for DP. Thus, increasing the contact surface, which facilitates diffusion into the pores during the adsorption process, the SEM analysis of OS found by Bohli et al. [16] and Ghouma et al. [17] is almost similar to that of present study. SEM micrographs of OS and DP show that the distribution of OS pores is somewhat homogeneous unlike DP, which presents few pores with some superficial heterogeneity, a similar result for DP is found by Sekirifa [18].

3.2. FTIR analysis

The OS and DP spectra are characterized by a main band corresponding to the groups of OH and NH with vibrations of valence from 3,424 to 3,416.8 cm^{-1}, same results have been reported by Aksas [19], the bands around 2,922.7–2,841.78 cm^{-1} for DP and non-existent for OS spectrum, correspond to the C–H/OH and C–H of CHO asymmetric valence vibrations that are similar to those found by Bohli et al. [16]. The bands from 1,666 to 1,600.4 cm^{-1} can be assigned to groups of C=O, in the following bands two ranges have been found: 1,666.0 cm^{-1} for OS and 1,600.4 cm^{-1} for DP, same peaks are found by Belhachemi et al. [20], which shows that the DP band decreases slightly compared with

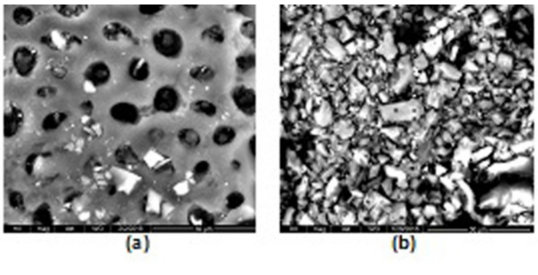

Fig. 1. SEM images of (a) OS and (b) DP.

that of OS. Peaks around 1,589.1–1,564.1 cm^{-1} for OS which are decreased to 1,493.2–1,432.9 cm^{-1} for DP are attributed to the C–H bond, C=O amide and N–H.

The 1,225.4 cm^{-1} band of OS which corresponds to the vibrations of the OH and NO_2 function with bands of 1,188.6–1,077.9 cm^{-1} of DP indicate the presence of C–OH primary alcohol and CN elongation bonds, similar results were found by Belhachemi et al. [20]. And finally the bands 906.7–696.3 cm^{-1} which characterize the two spectra of OS and DP corresponding to the C–H and C–N bonds.

These results allow us to observe that the OS bands have a slightly higher wave number than that of DP, contrary to the characteristic spectral intensity of the DP which is higher than that of OS (Fig. 2).

Table 1 presents the results obtained by FTIR for samples of OS and DP.

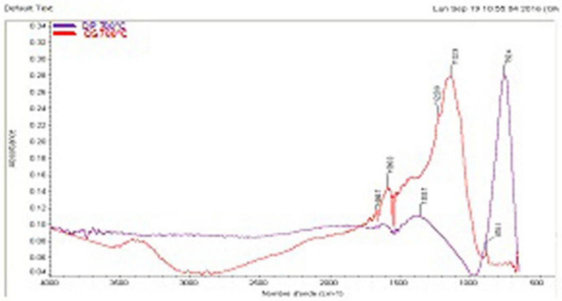

Fig. 2. FTIR data for olive stones and date pits.

Table 1
FTIR assignments of functional groups on OS and DP surface

Surface groups	Peak (cm^{-1})	
	OS 700°C	DP 700°C
OH/NH	3,416.8	3,424/3,060/3,026.8
C–H/OH	–	2,922.7/2,917.1
C–H of CHO	–	2,850
C=O	1,666.0	1,600.4
C–OH/C=O amide/N–H	1,589.1/1,564.1	1,493.2/1,452.9
OH/NO_2	1,225.4	–
C–H/C–O primary alcohol/C–N	–	1,188.6/1,151.9/1,077.9
C–H/N–H	869.9/706.5	906.7/756.5/696.3

3.3. Chemical analysis by X-ray fluorescence

Table 2 and Fig. 3 show that the material treated is composed mainly of calcium (87.48% for OS and 20.36% for DP) and potassium (7.13% for OS and 60.16% for DP).

In view of the mentioned results, according to this study, the OS are the richest in calcium, similar results are found by Ghouma et al. [17], in addition, the DP have a higher potassium content indicating that the surface of the coals is of a potash nature. The P and S with Si detected on the surface of DP and OS, respectively, are present in low concentrations.

3.4. Influence of solution pH

The pH of the solution is a key factor that could affect the adsorption of a drug on an adsorbent [21]. The adsorption capacity of PAC onto OS and DP as a function of initial pH of 2–11 is presented in Fig. 4.

Table 2
Chemical analysis of OS and DP by X-ray fluorescence

Mass %	OS	DP
Si	5.39	1.82
P	–	15.24
S	–	2.42
K	7.13	60.16
Ca	87.48	20.36
Mn	–	–
Fe	–	–

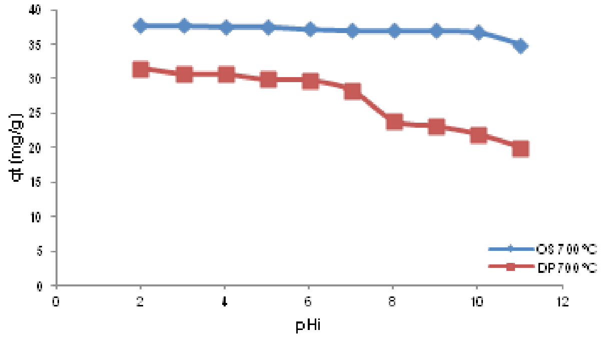

Fig. 4. Adsorption of paracetamol (PAC) on olive stone (OS) and date pit (DP) as a function of initial pH after 3 h contact time, sorbent amount 10 mg, T 20°C, PAC initial concentration 100 µM.

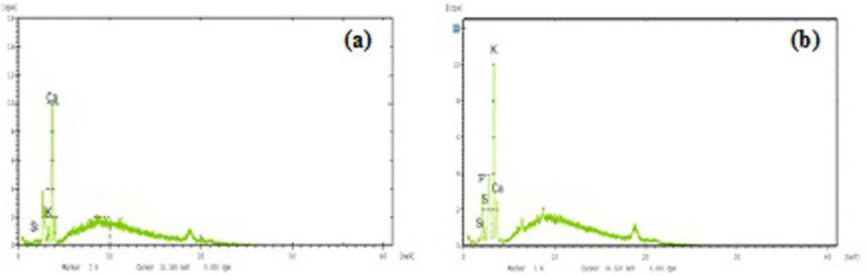

Fig. 3. Chemical analysis graphs of (a) OS and (b) DP by X-ray fluorescence.

As shown in Fig. 4, the adsorption capacity did not significantly change by alternating the pH value and shows the higher adsorption capacity of OS compared with the percentage of PAC removed by DP. The adsorption capacity of PAC decreased very slowly from 37.76 to 36.99 mg g^{-1} and 31.15 to 23.10 mg g^{-1} for OS and DP, respectively. With the pH increase from 2 to 9. But, with further increases of pH up to 12, the adsorption capacity declined considerably from 36.99 to 34.90 mg g^{-1} and from 23.10 to 20.03 mg g^{-1} for OS and DP, respectively.

The results presented in Fig. 4 put into evidence that PAC adsorption onto the studied sorbents is not dependent on pH as the adsorption capacity of PAC by OS and DP is equal for all the tested initial pHs. In the case of DP, the decrease in adsorption capacity observed at initial pH higher than 7 can be justified by damaging the sorbent at so high pH values. Therefore, depending on the initial pH the adsorbents are partially positively or negatively charged and ready to interact electrostatically with any deionized sorbate. However, this is not the case of PAC as it possesses a pKa of 9.38, and therefore in the studied range of pH it is mostly in its molecular form [15]. Similar observation was reported by Villaescusa et al. [22], PAC paracetamol sorption onto cork bark, yohimbe bark and grape stalk sorbents was not depended on pH; since there was minimal change in the sorption capacity it is clear that electrostatic interactions are not responsible for PAC adsorption onto the sorbents.

According to the literature, for example, the adsorption of norfloxacin and acetaminophen (ACE) by animal hair-based activated carbon, the ACT (PAC) adsorption had a constant rate from 88% to 92% at the pH of 2–9; but, in a higher pH range, the removal efficiency was significantly decreased by 70% [23]. In another research performed by Mashayekh-Salehi and Moussavi [24], the sorption of ACE by NH_4Cl^- induced activated carbon did not significantly change by alternating the pH value (decreased very slowly from 90% to 83%). But, with further increases of pH up to 12, the adsorption capacity declined to 70%. In another study [25], it was observed that for pH values from 3 to 10, the percentage removal for PAC onto magnetic activated carbon C-1 was practically constant within this pH interval.

For the treatment with adsorption, it is not necessary to make any pH adjustments if the solution of the effluent is within pH 2.0–9.0. This result also reveals that the mechanism of adsorption of PAC in OS and DP process can perform at natural pH of the solution and for full scale application. So, this process will be more cost-effective than other pharmaceutical compounds adsorption mechanisms which may need acidic or basic agents for attaining proper pH level. Almost all the researchers have similarly reported the nearly constant adsorption of ACT by different adsorbents in the pH range of 2–10 [24].

For this reason, all the solutions were prepared in natural pH of the solution pH 6.

3.5. Effect of temperature

The influence of temperature on the adsorption capacity of PAC in OS and DP is shown in Fig. 5. For these two adsorbents and after a time of 150 min, it was found that the adsorption capacity decreased with the temperature increase from 37.12 mg g^{-1} at 20°C to 36.31 mg g^{-1} at 40°C for OS and 29.74 mg g^{-1} at 20°C to 28.65 mg g^{-1} at 40°C for DP (Table 4) and even the adsorption capacity obtained by the OS is greater than that obtained by the DP for different studied temperatures. This shows that the adsorption was exothermic and the decrease of the adsorption capacity of the PAC with the increase in temperature is due to the increase in the solubility of the adsorbate (PAC), which has hampered the adsorption because the drug would have more affinity with the solvent than with the adsorbent.

As the temperature increases, the attraction forces between the surface of the adsorbents and the PAC ion are weakened and the sorption decreases [26].

3.6. Kinetic study

Several kinetic models have been proposed to clarify the mechanism of a solute sorption from aqueous solution onto an adsorbent: (a) a pseudo-first-order and the pseudo-second-order kinetic model, based on solid phase sorption [27,28] and (b) intra-particle diffusion model was also used as a first approach for identifying the limiting adsorption step and the diffusion/transport mechanisms during solute adsorption [29].

First, the adsorption kinetics of PAC for OS and DP was evaluated using the linearized pseudo-second-order equation (Eqs. (2) and (3))as follows:

$$\log\left(q_e - q_t\right) = \log q_e - \frac{k_1}{2.303}t \tag{2}$$

$$\frac{t}{q_t} = \frac{1}{k_2 q_e^2} + \frac{1}{q_e}t \tag{3}$$

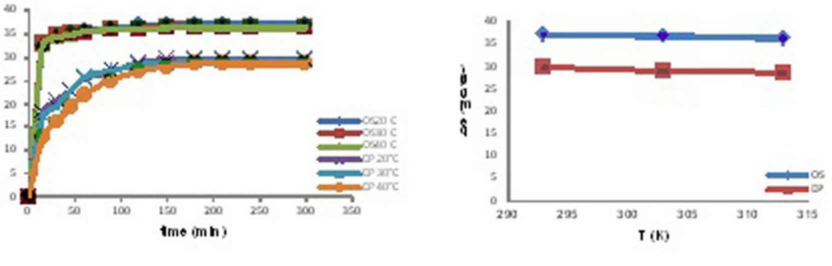

Fig. 5. Effect of temperature on adsorption of PAC. *T* (20°C, 30°C and 40°C), sorbent amount 10 mg, initial pH 6.0, initial concentration 100 μM and contact time 3 h.

where k_1 and k_2 are the pseudo-first-order (h^{-1}) and pseudo-second-order ($g\ mg^{-1}\ h^{-1}$) rate constant, q_e and q_t are the adsorbate uptake ($mg\ g^{-1}$) at equilibrium and at time t, respectively. $h = k_2 q_e^2$ ($mg\ g^{-1}\ min^{-1}$) represents the initial adsorption rate.

Intra-particle diffusion model can be expressed as follows:

$$q_t = K_{\text{int}} t^{\frac{1}{2}} + C \tag{4}$$

where K_{int} is the intra-particle diffusion rate constant ($mg\ g^{-1}\ min^{-0.5}$) and C ($mg\ g^{-1}$) represents the thickness of the boundary layer [29]. The diffusion coefficient, D, for the intra-particle transport of PAC was also calculated using the following equation [30]:

$$D = \frac{\pi}{8{,}640}\left(\frac{\text{d}p.K_i}{q_e}\right)^2 \tag{5}$$

Table 3 presents the evaluated parameters of the kinetic models for the adsorption of PAC in the two adsorbents. The adsorption process follows the pseudo-second-order kinetics for OS and DP (Fig. 6(a)) because the obtained coefficients of determination (R^2) are closer to unity. The theoretical values of q_e were similar to those obtained experimentally (Table 3) compared with those obtained by pseudo-first-order kinetics which were very unfavorable. As a result, the values of q_e, the rate constant, k_2, and the initial adsorption rate, h, found for OS (37.12 mg g^{-1}, 0.0128 g mg^{-1} min^{-1} and 17.63 mg g^{-1} min^{-1}, respectively) were significantly greater than those obtained for DP which were 29.74 mg g^{-1}, 0.0032 mg g^{-1} min^{-1} and 2.83 mg g^{-1} min^{-1}, respectively, certainly due to pore volumes (transport pores) of OS, which promotes adsorbate diffusion on the porous structure, this may occur because the motive force that has caused interaction with the active sites of the adsorbents has also increased [31].

In the present study, all plots were not adopted by origin (Fig. 6(b)). This indicates that intra-particle diffusion is not the only limiting step but also other kinetic models can control the rate of adsorption [32]. Two differentiated steps were detected for the adsorption of PAC in OS and DP: the curved initial part represents the diffusion of adsorbate in the boundary layer (external mass transfer). The second phase is the phase of progressive adsorption where the molecules of the adsorbate diffuse through the porosity of the adsorbent (intra-particle diffusion) until the equilibrium plateau is reached [33].

In both steps and from the values of K_i and D obtained for DP, these are higher than those obtained for OS, due to the adsorption sites available on the DP surface which are smaller compared with those available on OS that have a porous structure and also because of the low concentration of solution [34]. The results show that the intercept C values for OS are higher than those of DP (for the first step: 27.20 mg g^{-1} with 9.74 mg g^{-1} and for the second step 35.06 mg g^{-1} with 25.14 mg g^{-1} for OS and DP, respectively), this increase also provides a measure of the abundance of adsorbed solute on the boundary layer.

Table 3
Kinetic parameters for the adsorption of PAC onto olive stones and date pits

First-order kinetic model					Second-order kinetic model				
	$q_{e,\text{exp}}$ ($mg\ g^{-1}$)	$q_{e,\text{cal}}$ ($mg\ g^{-1}$)	$k_1\ 10^{-2}$ (min^{-1})	R^2	$q_{e,\text{cal}}$ ($mg\ g^{-1}$)	k_2 ($g\ mg^{-1}\ min^{-1}$)	h ($mg\ g^{-1}\ min^{-1}$)	R^2	R%
OS	37.12	14.04	8.24	0.901	37.45	0.0128	17.63	0.999	98.19
DP	29.74	24.69	7.16	0.948	30.95	0.0032	2.83	0.998	78.69
Intra-particle diffusion model									
	C_1 ($mg\ g^{-1}$)	D_1 ($cm\ min^{-1}$)	K_{i1} ($g\ mg^{-1}\ min^{-1}$)	R^2	C_2 ($mg\ g^{-1}$)	D_2 ($cm\ min^{-1}$)	K_{i2} ($g\ mg^{-1}\ min^{-1}$)	R^2	
OS	27.20	5.79×10^{-15}	1.186	0.939	35.06	7.28×10^{-17}	0.133	0.746	
DP	9.74	2.40×10^{-14}	1.937	0.975	25.14	5.54×10^{-16}	0.294	0.641	

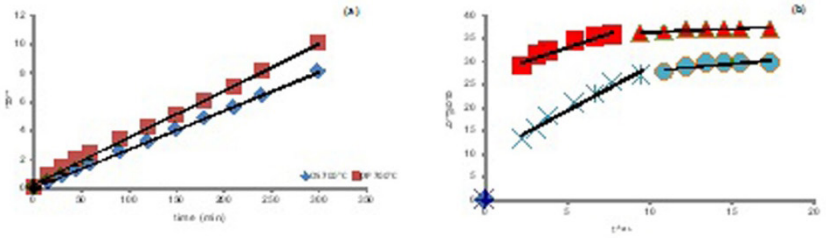

Fig. 6. Linear plots of (a) the pseudo-second-order and (b) intra-particle diffusion models for the removal of paracetamol by olive stones and date pits.

3.7. Adsorption isotherms

Equilibrium data, commonly known as adsorption isotherms, are basic requirements for the design of adsorption system [35]. In this study, the equilibrium data for PAC removal onto OS and DP were modeled with the Langmuir (Eq. (6)) [36] and Freundlich (Eq. (8)) [37] models.

$$\frac{C_e}{q_e} = \frac{1}{q_{\max}.K_L} + \frac{1}{q_{\max}}C_e \tag{6}$$

The essential characteristics of Langmuir isotherm can be expressed in terms of dimensionless separation factor, R_L given [38] by Eq. (7):

$$R_L = \frac{1}{1+K_L.C_0} \tag{7}$$

Freundlich isotherm presented an empirical isotherm equation can be written as follows:

$$\log q_e = \log K_F + \frac{1}{n}\log C_e \tag{8}$$

where K_L (L mg^{-1}) and K_F (L g^{-1}) are the Langmuir and Freundlich constants, respectively; $q_{\max}$ (mg g^{-1}) is a parameter related to the maximum amount of adsorbate required for monolayer formation; and n is a parameter related to the intensity of adsorption and to the system heterogeneity.

According to the classification of Giles et al. [39], the adsorption isotherms of PAC on OS and DP display an isotherm of the curve L (Fig. 7) characteristic of a steep initial rise and a curvature concave at low equilibrium concentrations typical of a plateau or saturation limit, indicating that several sites in the substrate are filled, it becomes more difficult for a molecule of unadsorbed solute (PAC) to find a vacant site [40].

Table 4 summarizes the parameters related to the Langmuir and Freundlich isotherm. The correlation coefficients obtained by the Langmuir isotherm using OS and DP are 0.989 and 0.998, respectively, representing the applicability of the Langmuir model under equilibrium conditions. The maximum absorption capacity for OS was 37.12 mg g^{-1} as an adsorbent, while in the case of DP it was 29.74 mg g^{-1}, indicating that OS had a greater adsorption capacity than DP. The R_L values were less than 1, indicating that adsorption is a favorable process [41].

The adsorption constant (K_F) and the adsorption intensity (n) were also studied. The calculated K_F values were 70.27 L g^{-1} for OS and 21.25 L g^{-1} for DP, showing appreciable affinity for PAC adsorption. The largest K_F value for OS indicates the same trend as found in the Langmuir isotherm, OS is more effective for the removal of PAC than DP. The (n) values for adsorption of PAC using OS and DP was 1.919 and 2.551, respectively. The value of (n) ranging from 1 to 10 shows favorable adsorption for both adsorbents and shows that the Freundlich model is applicable [42] and could be of physical nature [43] indicating good adsorption [44]. A comparison of the maximum experimental adsorption capacities between different adsorbents is given in Table 5. From these results, it is possible to verify that the activated carbon obtained from OS and DP has a good adsorption capacity in comparison with other adsorbents.

3.8. Thermodynamic study

Thermodynamic parameter such as Gibb's free energy ($\Delta G°$) for the adsorption of PAC on OS and DP was determined by using the following equation [28]:

$$\Delta G^{\circ}_{\text{ads}} = -RT\ln K \tag{9}$$

The K equilibrium constant, which represents the ratio between the concentration of solute that is adsorbed and

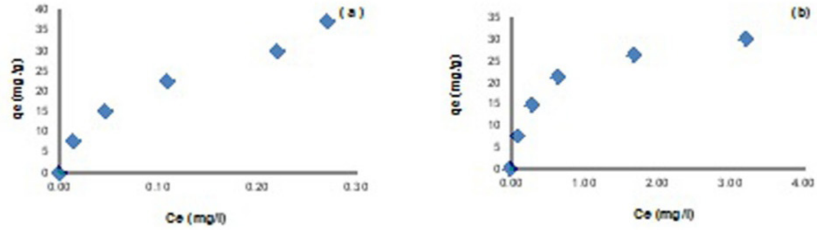

Fig. 7. Equilibrium adsorption isotherms of paracetamol sorption onto OS (a) and DP (b), paracetamol initial concentration (20–100 µM), sorbent amount 10 mg, initial pH 6.0, temperature 20°C and contact time 3 h.

Table 4
Equilibrium parameters for the adsorption of PAC onto OS and DP

Samples	Langmuir					Freundlich		
	$q_{e,\exp}$ (mg g^{-1})	$q_{e,\text{cal}}$ (mg g^{-1})	K_L (L mg^{-1})	R_L	R^2	$1/n$	K_F (L g^{-1})	R^2
OS 700°C	37.12	36.63	17.24	3.82×10^{-3}	0.989	1.919	70.27	0.992
DP 700°C	29.74	31.05	3.22	2.01×10^{-2}	0.998	2.551	21.25	0.943

Table 5
Summary of recently published literature on PAC adsorption by several activated carbon

Adsorbent	Experimental conditions	Observations	Adsorption capacity q_e	Models	References
B Box	T = 30°C C_0 = 120 mg dm^3 Dose of AC: 10 mg/15 cm^3	Coal B has obtained from physical activation Box obtained by chemical oxidation with ammonium persulfate	171 mg g^{-1} 87 mg g^{-1}	Intra-particle diffusion model	[45]
Vegetable wastes: Grape stalk, Yohimbe bark Cork bark	[C_0] = 20 mg L^{-1} T = 22°C ± 2°C V = 15 mL Carbon dose = 100 mg pH = 6 Time contact = 2 h	Vegetable wastes before being crushed and sieved to a particle size of 0.63–0.75 mm. After this procedure, the adsorbent was used without any physical or chemical pretreatment	2 mg g^{-1} 0.77 mg g^{-1} 0.99 mg g^{-1}	Langmuir	[22]
Vegetable wastes: Sugar cane bagasse (SCB) Vegetable sponge (VS)	pH = 7.0 [C_0] = 5 μmol Weight of activated carbon: 3 g D = 30 mL min^{-1}	Vegetable wastes were washed with water (pH 7.0) and then dried in a laboratory oven (60°C) for 15 h. In the next step, the material went to an industrial blender with posterior sieving to obtain particles sizes between 1.19 and 4.76 mm for SCB and VS, respectively	120.5 μg g^{-1} 37.5 μg g^{-1}	Langmuir	[2]
Sisal waste: S/0.5:1/700 S/0.5:1/800	T = 30°C C_0 = 120 mg dm^3 Weight of activated carbon: 10 mg/15 cm^3	Sisal waste was used as precursor to prepare carbons by chemical activation with K_2CO_3 and different temperatures (700°C and 800°C)	120.5 mg g^{-1} 124.5 mg g^{-1}	–	[46]
Carbon replica	200 rpm C_0 = 20 ppm/500 mL Dose of AC: 0.920 mg	Carbon replica has obtained from physical activation and chemical oxidation with H_2SO_4	2.989 mg g^{-1}	–	[47]
Dende coconut mesocarp	T = 25°C and 200 rpm C_0 = 20 cm^3 Dose of AC: 10 mg	The samples were previously washed with hot deionized water (50°C), dried in an incubator for 24 h at 60°C, ground and sieved with average diameter of 0.180 mm (70–100 mesh ASTM). No previous chemical or physical treatment was done	64.65 mg g^{-1}	Langmuir	[48]
Olive stone Date pit	[C_0] = 100 μM T = 22°C ± 2°C V = 15 mL Carbone dose = 10 mg pH = 6 Time contact = 3 h	Vegetable wastes were heat treated at 700°C without any physical or chemical pretreatment	37.12 mg g^{-1} 29.74 mg g^{-1}	Langmuir	Present study

Table 6
Thermodynamic parameters for paracetamol adsorption onto OS and DP at different temperatures

Samples	$q_{e,\mathrm{exp}}$ (mg g^{-1})			$\Delta G°$ (kJ mol^{-1})			$\Delta H°$ (kJ mol^{-1})	$\Delta S°$ (J mol^{-1} K^{-1})	R^2
	20°C	30°C	40°C	20°C	30°C	40°C			
OS 700°C	37.12	36.64	36.31	–9.74	–8.69	–8.33	–30.46	–71.07	0.961
DP 700°C	29.74	29.22	28.65	–3.18	–3.08	–2.97	–6.17	–10.21	0.999

the concentration of solute remaining in solution, can be calculated using the expression: $K = \frac{(C_i - C_e)}{C_e}$, the variation of enthalpy $\Delta H°$ and entropy $\Delta S°$ of adsorption is obtained from slope and intercept of a plot of ln$K$ vs. 1/T [28], is expressed by the following equation:

$$\ln K = \frac{\Delta S^{\circ}_{\mathrm{ads}}}{R} - \frac{\Delta H^{\circ}_{\mathrm{ads}}}{RT} \qquad (10)$$

where R is the universal gas constant (8.314 J mol^{-1} K^{-1}) and T is the absolute temperature (K). The calculated thermodynamic parameters are given in Table 6. The negative values of $\Delta G°$ (between 0 and –20 kJ mol^{-1}) are compatible with the electrostatic interaction between the adsorption sites and the adsorption ion (physical adsorption) [49] and indicates that the adsorption of PAC on OS and DP is a spontaneous process.

The exothermic nature is also indicated by the decrease in the amount of adsorption at increasing temperatures. In addition, the value of $\Delta H°$ for the OS was –30.46 kJ mol^{-1}, whereas in the case of DP it was –6.17 kJ mol^{-1}, indicating that the OS adsorption process is more exothermic compared with DP, and even the values obtained were less than 40 kJ mol^{-1}, suggesting a physical adsorption process [50] and confirming the exothermic nature [24]. Concerning the negative value of $\Delta S°_{\mathrm{ads}}$ ($\Delta S°$ = –71.07 J mol^{-1} K^{-1} for OS and $\Delta S°$ = –10.21 J mol^{-1} K^{-1} for DP), this suggests that the adsorption of PAC by DP is more random in the solid–solution interface compared with the OS [51].

4. Conclusion

Between the two wastes studied in this paper, olive stone has a high adsorption capacity of PAC compared with the performance of DP (98.19% for OS with 78% for the DP). The velocity control step was described by pseudo-second-order kinetics, and the adsorption isotherms were well determined by both the Langmuir and Freundlich models. When the temperature rises from 20°C to 40°C, a slight decrease in the adsorption capacity is observed, which shows that the process of adsorption of PAC is more exothermic, accompanied by a decrease in the randomness to the solid interface/solution compared with DP. Because of its better PAC adsorption capacity as well as its high availability at low cost, olive residue can be used as a sorption agent in sewage treatment plants in the same region (northern Algeria), and even can be removed after use by combustion under controlled conditions.

References

[1] M. Soufan, Oxydation par le chlore de composes pharmaceutiques, Thèse de doctorat, l'Université Poitiers, chimie et microbiologie de l'eau, 173, 2011 (Oxidation of Pharmaceutical Compounds by Chlorine, Doctoral Thesis, University Poitiers, Chemistry and Microbiology of Water, 173, 2011).
[2] A.V. Flores Nardy Ribeiro, M. Belisario, R. Moretto Galazzi, D. Cazoni Balthazar, Evaluation of two bioadsorbents for removing paracetamol from aqueous media, J. Biotechnol., 14 (2011) 1–10.
[3] J. Radjenovic, M. Petrovic, D. Barceló, Fate and distribution of pharmaceuticals in wastewater and sewage sludge of the conventional activated sludge (CAS) and advanced membrane bioreactor (MBR) treatment, Water Res., 43 (2009) 831–841.
[4] J. Rivera-Utrilla, M. Sánchez-Polo, M.Á. Ferro-García, G. Prados-Joya, R. Ocampo-Pérez, Pharmaceuticals as emerging contaminants and their removal from water. A review, Chemosphere, 93 (2013) 1268–1287.
[5] A. Jelic, M. Gros, A. Ginebreda, R. Cespedes-Sánchez, F. Ventura, M. Petrovic, D. Barcelo, Occurrence, partition and removal of pharmaceuticals in sewage water and sludge during wastewater treatment, Water Res., 45 (2011) 1165–1176.
[6] P. Verlicchi, M. Al Aukidy, E. Zambello, Occurrence of pharmaceutical compounds in urban wastewater: removal, mass load and environmental risk after a secondary treatment – a review, Sci. Total Environ., 429 (2012) 123–155.
[7] S. Cheng, J. Wu, H. Xia, J. Peng, S. Wang, L. Zhang, Microwave-assisted regeneration of spent activated carbon from paracetamol wastewater plant using response surface methodology, Desal. Wat. Treat., 57 (2016) 18981–18991.
[8] J. Lladó, C. Lao-Luque, B. Ruiz, E. Fuente, M. Solé-Sardans, A.D. Dorado, Role of activated carbon properties in atrazine and paracetamol adsorption equilibrium and kinetics, Process Saf. Environ. Prot., 95 (2015) 51–59.
[9] Y. Kim, K. Choi, J. Jung, S. Park, P.-G. Kim, J. Park, Aquatic toxicity of acetaminophen carbamazepine, cimetidine, diltiazem and six major sulfonamides, and their potential ecological risks in Korea, Environment Int., 33 (2007) 370–375.
[10] The State of Food and Agriculture, FAO STATE, 2013.
[11] The official website of the International Exhibition of the Dating of Biskra "SIDAB", whose first edition was organized from 21 to 24 march in Biskra under the auspices of the Zibans Chamber of Commerce and Industry and the Algerian Chamber of Commerce and Industry, 2015.
[12] H. Babaci, H. Aksas, K. Louhab, Biosorption of anionic dye Bezaktiv Yellow HE-4G on mixture of olive stone and date pits in backed bed column, Asian J. Chem., 27 (2015) 4029–4033.
[13] N. Babakhouya, S. Boughrara, F. Abed, N. Abai, S. Midoune, Etude du potentiel d'utilisation des déchets agroalimentaires, les grignons d'olives et les noyaux de date pour recuperation et adsorption des métaux lourds, Algerian J. Environ. Sci. Technol., 1 (2015). ISSN: 2437-1114.
[14] A. Chouchene, Etude expérimentale et théorique de procédés de valorisation de sous produits oléicoles par voies thermique et physico-chimique, Food and Nutrition, University Haute Alsace, Mulhouse, 2012 (Experimental and theoretical study of processes for the valorization of sub-olive products by thermal and physico-chemical means).

[15] O. Lorphensri, J. Intravijit, D.A. Sabatini, T.C.G. Kibbey, K. Osathaphan, C. Saiwan, Sorption of acetaminophen, 17α-ethynyl estraiol, nalidixic acid, and norfloxacin to silica, alumina, and a hydrophobic medium, Water. Res., 40 (2006) 1481–1491.

[16] T. Bohli, A. Ouederni, N. Fiol, I. Villaescusa, Evaluation of an activated carbon from olive stones used as an adsorbent for heavy metal removal from aqueous phases, C.R. Chim. (2014) 1–12.

[17] I. Ghouma, M. Jeguirim, S. Dorge, L. Limousy, C.M. Ghimbeu, A. Ouederni, Activated carbon prepared by physical activation of olive stones for the removal of NO_2 at ambient temperature, C.R. Chim. (2014) 1–12.

[18] M.L. Sekirifa, Étude des propriétés absorbantes des charbons activés issus des noyaux de dattes, Application au traitement d'effluent aqueux, une thèse de doctorat, 2013 (Study of the Absorbent Properties of Activated Carbons from Date Pits. Application to the Treatment of Aqueous Effluent, Doctoral Thesis, Badji Mokhtar –Annaba University, 2013).

[19] H. Aksas, Etude cinétique et thermodynamique de l'adsorption des métaux lourds par l'utilisation des adsorbants naturels (Kinetic and Thermodynamic Study of the Adsorption of Heavy Metals by the Use of Natural Adsorbents), Doctoral Thesis, Boumerdes University, Algérie, 198, 2012.

[20] M. Belhachemi, M. Jeguirim, L. Limousy, F. Addoun, Comparison of NO_2 removal using date pits activated carbon and modified commercialized activated carbon via different preparation methods: effect of porosity and surface chemistry, Chem. Eng. J., 253 (2014) 121–129.

[21] V. Arya, L. Philip, Adsorption of pharmaceuticals in water using Fe_3O_4 coated polymer clay composite, Microporous Mesoporous Mater., 232 (2016) 273–280.

[22] I. Villaescusa, N. Fiol, J. Poch, A. Bianchi, C. Bazzicalupi, Mechanism of paracetamol removal by vegetable wastes: the contribution of p–p interactions, hydrogen bonding and hydrophobic effect, Desalination, 270 (2011) 135–142.

[23] H. Liu, W. Ning, P. Cheng, J. Zhang, Y. Wang, C. Zhang, Evaluation of animal hairs-based activated carbon for sorption of norfloxacin and acetaminophen by comparing with cattail fiber-based activated carbon, J. Anal. Appl. Pyrolysis, 101 (2013) 156–165.

[24] A. Mashayekh-Salehi, G. Moussavi, Removal of acetaminophen from the contaminated water using adsorption onto carbon activated with NH_4Cl, Desal. Wat. Treat., 57 (2016) 12861–12873.

[25] C. Saucier, P. Karthickeyan, G.S. dos Reis, V. Ranjithkumar, I.A.S. de Brum, E.C. Lima, Efficient removal of amoxicillin and paracetamol from aqueous solutions using magnetic activated carbon, Environ. Sci. Pollut. Res., 24 (2017) 5918–5932.

[26] M. Antunes, V.I. Esteves, R. Guégan, J.S. Crespo, A.N. Fernandes, M. Giovanela, Removal of diclofenac sodium from aqueous solution by Isabel grape bagasse, Chem. Eng. J., 192 (2012) 114–121.

[27] Y.S. Ho, Review of second-order models for adsorption systems, J. Hazard. Mater., 136 (2006) 681–689.

[28] Y. Önal, C.A.R. Akmil-Bas, Ç. Sar1c1-Özdemir, Elucidation of the naproxen sodium adsorption onto activated carbon prepared from waste apricot: kinetic, equilibrium and thermodynamic characterization, J. Hazard. Mater., 148 (2007) 727–734.

[29] W.J. Weber, J.C. Morris, Kinetics of adsorption on carbon from solution, J. Sanit. Eng. Div. ASCE, 89 (1963) 31–60.

[30] G.H. Pino, L.M.S. Mesquita, M.L. Torem, G.A.S. Pinto, Biosorption of cadmium by green coconut shell powder, Miner. Eng., 19 (2006) 380–387.

[31] S.K. Bajpai, M. Bhowmik, Adsorption of diclofenac sodium from aqueous solution using polyaniline as a potential sorbent. I. Kinetic studies, J. Appl. Polym. Sci., 117 (2010) 3615–3622.

[32] M. Kilic, E. Apaydin-Varol, A.E. Putun, Adsorptive removal of phenol from aqueous solutions on activated carbon prepared from tobacco residues: equilibrium, kinetics and thermodynamics, J. Hazard. Mater., 189 (2011) 397–403.

[33] C. Valderrama, X. Gamisans, F.X. las Heras, J.L. Cortina, A. Farran, Kinetics of polycyclic aromatic hydrocarbons removal using hyper-cross-linked polymeric sorbents Macronet Hypersol MN200, React. Funct. Polym., 67 (2007) 1515–1529.

[34] S. Venkata Mohan, N. Chandrasekhar Rao, J. Karthikeyan, Adsorption removal of direct azodye from aqueous phase onto coal based sorbents – a kinetic and mechanistic study, J. Hazard. Mater., 90 (2002) 189–204.

[35] A. Ozer, G. Dursun, Removal of methylene blue from aqueous solution by dehydrated wheat bran carbon, J. Hazard. Mater., 146 (2007) 262–269.

[36] I. Langmuir, The adsorption of gases on plane surfaces of glass, mica and platinum, J. Am. Chem. Soc., 40 (1918) 1361–1367.

[37] H.M.F. Freundlich, Over the adsorption in solution, J. Phys. Chem., 57 (1906) 385–470.

[38] Y.S. Ho, C.T. Huang, H.W. Huang, Equilibrium sorption isotherm for metal ions on tree fern, Process Biochem., 37 (2002) 1421–1430.

[39] C.H. Giles, T.H. Macewan, S.N. Nakhwa, D. Smith, Studies in adsorption. Part XI. A system of classification of solutions adsorption isotherms, and its use in diagnosis of adsorption mechanisms and in measurement of specific surface areas of solids, J. Chem. Soc., (1960) 3973–3993.

[40] R. Baccar, M. Sarra, J. Bouzid, M. Fiki, P. Blanquez, Removal of pharmaceutical compounds by activated carbons prepared from agricultural by-product, Chem. Eng. J., 211–212 (2012) 310–317.

[41] B.H. Hameed, A.T.M. Din, A.L. Al Ahmed, Adsorption of methylene blue onto bamboo-based activated carbon: kinetics and equilibrium studies, J. Hazard. Mater., 141 (2007) 819–825.

[42] B.H. Hameed, Evaluation of papaya seeds as a novel non-conventional low-cost adsorbent for removal of methylene blue, J. Hazard. Mater., 162 (2009) 939–944.

[43] A. Behnamfard, M.M. Salarirad, Equilibrium and kinetic studies on free cyanide adsorption from aqueous solution by activated carbon, J. Hazard. Mater., 170 (2009) 127–133.

[44] T. Mukoko, M. Mupa, U. Guyo, F. Dziike, Preparation of rice hull activated carbon for the removal of selected pharmaceutical waste compounds in hospital effluent, J. Environ. Anal. Toxicol. (2015) S7.

[45] B. Ruiz, I. Cabrita, A.S. Mestre, J.B. Parra, J. Pires, A.P. Carvalho, C.O. Ania, Surface heterogeneity effects of activated carbons on the kinetics of paracetamol removal from aqueous solution, Appl. Surf. Sci., 256 (2010) 5171–5175.

[46] A.S. Mestre, A.S. Bexiga, M. Proença, M. Andrade, M.L. Pinto, I. Matos, I.M. Fonseca, A.P. Carvalho, Activated carbons from sisal waste by chemical activation with K_2CO_3: kinetics of paracetamol and ibuprofen removal from aqueous solution, Bioresour. Technol., 102 (2011) 8253–8260.

[47] P. Pandey, V. Kumar Saini, Synthesis of low cost carbon replica for paracetamol removal from waste water and effect of temperature on adsorption capacity, Int. J. Occup. Health Saf. Fire Environ. Allied Sci., 5 (2015) 17–19.

[48] R.C. Ferreira, O.M. Couto Jr., K.Q. Carvalho, P.A. Arroyo, M.A.S.D. Barros, Effect of solution pH on the removal of paracetamol by activated of dende coconut mesocarp, Chem. Biochem. Eng. Q., 29 (2015) 47–53.

[49] D. Sigh, Studies of the adsorption thermodynamics of oxamymyl on fly ash, Adsorpt. Sci. Technol., 18 (2000) 742–748.

[50] B.K. Nandi, A. Goswami, M.K. Purkait, Adsorption characteristics of brilliant green dye on kaolin, J. Hazard. Mater., 161 (2009) 387–395.

[51] M.K. Purkait, A. Maiti, S. DasGupta, S. De, Removal of congo red using activated carbon and its regeneration, J. Hazard. Mater., 145 (2007) 287–295.